Synthesis, DNA Binding and Cytotoxicity of New Pyrazole Emodin Derivatives

ARTICLE *in* EUROPEAN JOURNAL OF MEDICINAL CHEMISTRY · OCTOBER 2006

Impact Factor: 3.45 · DOI: 10.1016/j.ejmech.2006.04.006 · Source: PubMed

7 AUTHORS, INCLUDING:

Jia-Heng Tan
Sun Yat-Sen University
84 PUBLICATIONS **1,333** CITATIONS
SEE PROFILE

Jianyong Wu
The Hong Kong Polytechnic University
112 PUBLICATIONS **2,369** CITATIONS
SEE PROFILE

Available online at www.sciencedirect.com
ScienceDirect
European Journal of Medicinal Chemistry 41 (2006) 1041–1047
EUROPEAN JOURNAL OF MEDICINAL CHEMISTRY
http://france.elsevier.com/direct/ejmech

Original article

Synthesis, DNA binding and cytotoxicity of new pyrazole emodin derivatives

J.-H. Tan [a], Q.-X. Zhang [b], Z.-S. Huang [a], Y. Chen [a], X.-D. Wang [a,b], L.-Q. Gu [a,*], J.Y. Wu [b,*]

[a] *School of Pharmaceutical Sciences, Sun Yat-Sen University, Guangzhou 510080, China*
[b] *Department of Applied Biology and Chemical Technology and the State Key Lab of Chinese Medicine and Molecular Pharmacology, the Hong Kong Polytechnic University, Hung Hom, Kowloon, Hong Kong*

Received in revised form 17 April 2006; accepted 20 April 2006
Available online 22 May 2006

Abstract

A series of new anthrapyrazoles were derived from emodin by attaching various cationic alkyl amino side chains onto a pyrazole ring which had been incorporated into the anthraquinone chromophore. Compared with emodin, the derivatives had significantly higher DNA binding affinity based on interaction with calf thymus DNA, and much more potent cytotoxicity against different tumor cells. The derivatives with a mono-cationic alkyl side chain exhibited the highest DNA binding affinity and cytotoxicity.

Keywords: Emodin derivatives; Anthrapyrazole; Amino side chain; DNA binding; Cytotoxicity; Tumor cells

1. Introduction

Chemical modification of bioactive components of medicinal herbs is one of the most common approaches in drug discovery for new drugs and improved therapeutic properties. Emodin (Fig. 1) is the major bioactive compound of numerous herb species such as *Rheum* and *Polygonum* (Polygonaceae), *Rhamnus* (Rhamnaceae) and *Senna* (Cassieae) [1]. It exhibits a variety of biological effects such as anti-inflammatory, antibiotic, antiviral and antineoplastic [2–5] activities. Moreover, it has been shown to inhibit the growth of various cancer cells [5–7], and induce the apoptosis of certain cancer cells [6,7].

Emodin belongs to the same class of coplanar anthraquinones as daunorubicin and mitoxantrone, which have been in clinical use over 30 years for the treatment of various tumors [8]. Their function as noncovalent DNA binders is generally believed to be essential for their activity. Most DNA binding compounds share two common structural features which appear to contribute to their activity, the presence of planar polycyclic aromatic systems and the occurrence of one or two side chains containing polymethyleneamine or sugar fragments in a strictly defined orientation to the chromophore. They interact with DNA via intercalative association and binding locations (minor groove, major groove, backbone, etc.), which may induce conformational changes in the regular helical structure, unwinding the DNA at the binding site and interfering with the function of DNA binding enzymes such as DNA topoisomerases and DNA polymerases [9–11]. The inhibition of topoisomerase II, in particular, has been established as the chief mechanism of action for the antitumor and cytotoxic effects of daunorubicin, mitoxantrone and related anthraquinones. The inhibition of topoisomerase II eventually leads to DNA double-strand breaks in the tumor cells and possibly, cell death. Although daunorubicin and mitoxantrone have excellent DNA binding and antitumor activities, they have shown serious side effects during cancer therapy, especially cardiotoxicity [8,12]. Various semi-synthetic approaches have been exercised to derive anthraquinone analogues with enhanced antitumor activities and reduced side effects. Some anthrapyrazole derivatives such as losoxantrone have shown potent antitumor activity on a number of tumor cell lines (including solid tumors) and lower cardiotoxicity [13–15].

Emodin itself has low DNA binding affinity, and low or insignificant cytotoxicity against various cancer cells [16]. Because of its coplanar structure, the incorporation of a pyrazole ring into its anthraquinone chromophore may increase the elec-

* Corresponding authors.
E-mail addresses: cedc42@zsu.edu.cn (L.-Q. Gu), bcjywu@polyu.edu.hk (J.Y. Wu).

0223-5234/$ - see front matter © 2006 Elsevier SAS. All rights reserved.
doi:10.1016/j.ejmech.2006.04.006

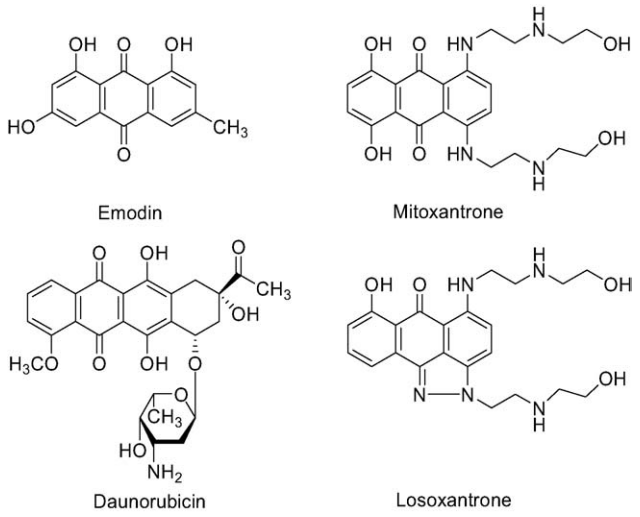

Fig. 1. Emodin, daunorubicin, mitoxantrone and losoxantrone molecular structures.

tron density of the π system area, which makes the chromophore more resistant to enzymatic reduction to radical species, thus to lower the cardiotoxicity [17]. The chromophore alone is not sufficient, however, the addition of side chains such as polymethyleneamine, sugar or heterocyclic to the chromophore, is usually effective to gain higher DNA binding affinity and antitumor activities [18,19]. The cationic amino side chains are most desirable as their distal amino group binds electrostatically to the phosphate moieties of DNA [18,20]. Moreover, chains of varying length, polarity, rigidity, charge and steric bulk may confer different DNA binding affinities.

This work aims to synthesize a group of new emodin derivatives with improved DNA binding affinity and antitumor activity by incorporating a pyrazole ring into the anthraquinone chromophore, and then attaching various cationic amino side chains to the pyrazole ring. The DNA binding capacity of the new anthrapyrazoles derived from emodin was evaluated based on interaction with calf thymus (CT) DNA, and their cytotoxicity was assessed on three types of tumor cell lines, mouse melanoma B16, human hepatocellular carcinoma HepG2, and Lewis lung carcinoma (LLC) cells. The molecular structure and bioactivity relationships were discussed.

2. Results and discussion

2.1. Synthesis of emodin derivatives

The synthetic steps of the target compounds are shown in Fig. 2. The starting compound emodin **1** was methylated to corresponding di-*O*-methyl emodin **2** at the specified conditions. Methylation of **1** yielded 6,8-*O*-dimethyl emodin **2** as the major product together with a very small amount of 3,8-*O*-dimethyl isomer. Then, 6,8-*O*-dimethyl emodin was purified by flash chromatography and crystallization. Compound **2** was converted to the corresponding tosylate **3**, and further treatment of **3** with 2-hydroxyethylhydrazine gave compound **4**, which was purified by column chromatography [21–23], and its structural assignment was confirmed with the nuclear Overhauser enhancement spectroscopy (NOESY) experiment. The methylene side chain adjacent to the pyrazole ring possessed NOEs with the 3-aromatic proton but not the 10-methoxy group. Compound **4** was further converted to the corresponding mesylate **5**. The target compounds **6**–**13** were attained by nucleophilic substitution of **5** with appropriate substituted amines (Fig. 3).

The emodin derivatives can be divided into three groups based on their amino side chains, a mono-cationic alkyl group (**6**–**8**), a di-cationic alkyl group (**9**, **10**) and a heterocycle substituent group (**11**–**13**). The free base forms of compounds **6**–**13** were converted into hydrochloride salts by treatment with hydrochloride acid in ethanol to enhance the chemical stability and solubility for the following biochemical assays.

2.2. DNA binding properties

The DNA binding properties of compounds **6**–**13** were evaluated based on their affinity or interaction with CT DNA, measured with absorption and fluorescence spectrometric titration [24,25]. Fig. 4 shows the representative absorption spectra of compound **6** (30 μM) in the presence of increasing concentrations of CT DNA (0–165 μM). Other compounds exhibited the similar absorption spectra pertaining to the chromophore but with the hypochromicity and red shifts dependent on the cationic amino side chains. These results were consistent with the

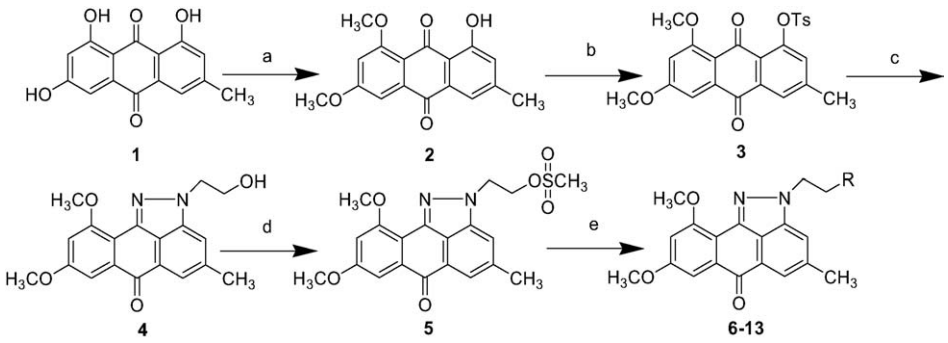

Fig. 2. Synthesis of anthrapyrazole derivatives with carboxamide side chains from emodin. Reagents: (a) Me_2SO_4, K_2CO_3, Me_2CO (room temperature); (b) *p*-toluenesulfonyl chloride, K_2CO_3, Me_2CO (reflux); (c) 2-hydroxyethylhydrazine, 2-ethoxyethanol (120 °C); (d) methanesulfonyl chloride, Et_3N, CH_2Cl_2; (e) N,N-dialkylaminoethylamine, ethanol (reflux).

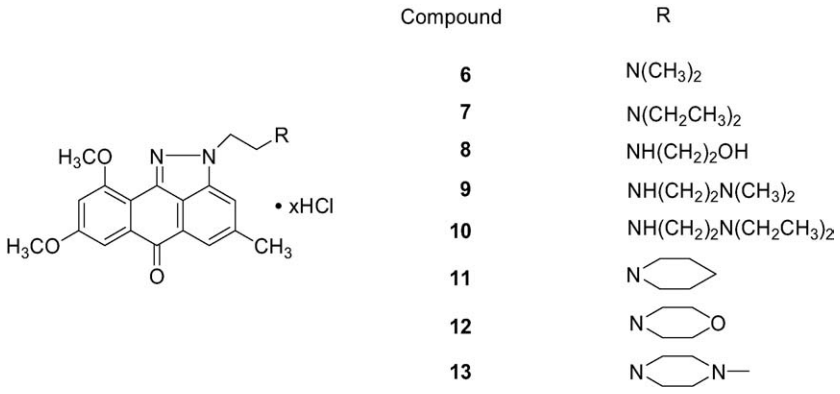

Fig. 3. Structures of emodin derivatives **6**–**13** from the synthetic steps shown in Fig. 2.

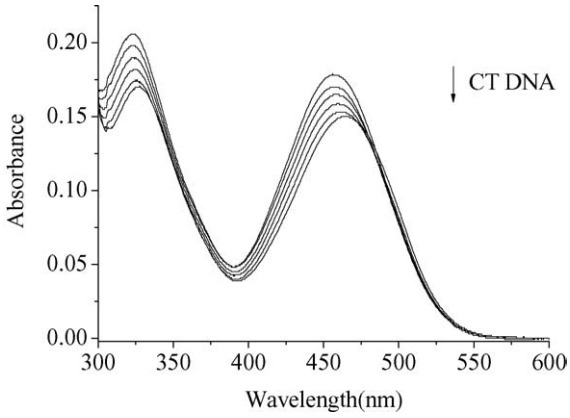

Fig. 4. Absorbance titration of **6** at 30 μM in 20 mM sodium phosphate buffer (pH 6.3) with 150 mM NaCl at increasing CT DNA concentration (arrow: 0–165 μM).

previous reports on the absorption titration of anthrapyrazole derivatives, and the hypochromicity of anthrapyrazoles in the presence of DNA is believed to be a result of their interactions with the DNA [26]. On the other hand, the red shift is associated with a decrease in the energy gap between the highest occupied molecular orbital (HOMO) and the lowest occupied molecular orbital (LUMO) when the drug binds to DNA [27].

The selection of ionic strength (150 mM NaCl) in the absorption titration experiments was mainly based on the avoidance of DNA deposition (or precipitation) in all drug solutions (30 μM). In the fluorescence spectrometric titration, a much lower drug concentration (3 μM) could be used at a lower NaCl concentration (20 mM) to measure the appropriate binding constants. Fig. 5a shows the fluorescence spectrometric titration spectra of compound **6**, and Fig. 5b the corresponding peak fluorescence intensity at increasing CT DNA concentration. The titration spectra and peaks for other compounds exhibited the similar trend of changes with the CT DNA concentration. The large increase in the fluorescence intensity with CT DNA concentration is suggestive of a strong association of the compound molecules with the DNA molecules. The association may shield the DNA molecules from the solvent molecules, leading to an increase in the emission intensity [28].

Table 1 summarizes the DNA binding constants and related properties of emodin and compounds **6**–**13** after interaction

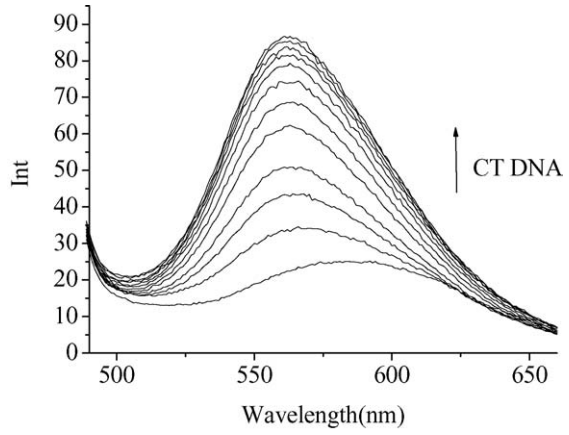

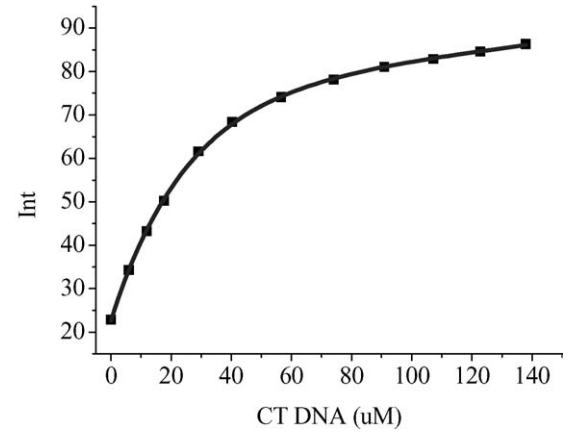

Fig. 5. (a) Fluorescence spectra of compound **6** at 3 μM in 20 mM sodium phosphate buffer (pH 6.3) with 20 mM NaCl at increasing CT DNA concentration (arrow: 0–138 μM); (b) the peak fluorescence intensity in (a) at 565 nm versus CT DNA concentration.

with CT DNA. The relative binding affinities as indicated by the binding constants K_i are in the order of **8** > **13** > **6** > **7** > **11** > **9** > **10** > **12** > emodin. Therefore, all derivatives had a higher DNA binding constant than their lead compound. This result indicates that introduction of the pyrazole ring and cationic amino side chains can dramatically increase the DNA binding capacity of emodin. Among the deri-

Table 1
Binding constants (K_i) and photometric properties of emodin and its derivatives **6**–**13** in contact with CT DNA

Compound	K_i ($\times 10^{-5}$ M^{-1})[a,c]	λ_{max} (nm)	Red shift (nm)[b,d]	Hypochromicity (%)[b,d]	Isosbestic point (nm)
Emodin	0.68	446	1	3	458
6	6.09	456	9	18	484
7	5.52	457	9	18	485
8	7.47	459	6	15	482
9	3.76	463	5	11	Unclear
10	2.53	465	4	13	Unclear
11	4.09	458	11	20	482
12	2.25	464	2	7	Unclear
13	6.98	467	4	13	496

[a] Three micromolars drug in 20 mM NaH_2PO_4-Na_2HPO_4 pH 6.3 buffer containing 20 mM NaCl at room temperature.
[b] Thirty micromolars drug in 20 mM NaH_2PO_4–Na_2HPO_4 pH 6.3 buffer containing 150 mM NaCl at room temperature.
[c] Obtained from spectrofluorimetric titration at $\lambda_{ex} = 410$ nm and $\lambda_{em} = 565$ nm.
[d] Obtained at λ_{max}.

vatives, those with stronger DNA binding affinities, **6**, **7**, **8**, **11** and **13** exhibited hypochromicity, red shifts and clear isobestic points. The spectral changes are suggestive of intercalative association as a major binding mode for these derivatives with CT DNA [29,30]. In contrast, compounds **9**, **10**, **12** exhibited no clear isobestic point, suggesting a different or a mixture of DNA binding modes for these low-affinity compounds.

Compound **8** which has the same side chain as mitoxantrone and losoxantrone had the largest DNA binding constant, which may be attributed to the strong binding of DNA molecules though electrostatic interaction and hydrogen bonding by its secondary amino and hydroxyl groups. The other derivatives **6**, **7**, **11** bearing mono-cationic side chains also exhibited significant binding capacity with the relative binding affinities in the order of **6** > **7** > **11**. The more bulky group with distal amine appears to have a lower DNA binding affinity. In the di-cationic alkyl group, much longer and more flexible ligands **9**, **10** showed weaker binding properties. Side chain flexibility and the two adjacent cationic centers may obstruct the chromophore from accessing the DNA base pairs, which may be responsible for the lower binding affinity compared with the mono-cationic compounds [31]. However, a higher binding affinity was observed in the more rigid compound **13**, which may be explained by that the rigid piperazine group can attach onto the major groove of DNA when the chromophore is inserted into the DNA base pairs [10,31]. Finally, the lower binding affinity of compound **12** may be attributed to the low pK_a value of its morpholine group.

2.3. Cytotoxicity against tumor cells

Table 2 shows the IC_{50} values (cytotoxicity potency indexes) of compounds **6**–**13** against three types of tumor cells in culture. The lead compound emodin exhibited low or insignificant cytotoxicity with high IC_{50} values, 55 μM on HepG2 cell and more than 100 μM on the other two cell lines. In comparison, all the derivatives had much more potent cytotoxicity with significantly lower IC_{50} values on most of the tumor cells. Of all the derivatives, compounds **6**, **7**, **8** were most potent in inhibiting the tumor cell proliferation with the lowest IC_{50} values of 1.7–5.0 μM. Likewise, these compounds also had relatively large DNA binding constants (Table 1). Therefore, the higher cytotoxic activity against the tumor cells may be attributed, at least in part, to their intercalative association and high binding affinity with the DNA of tumor cells. As for the structure–activity relationship, compounds **6**, **7**, **8**, **11** bearing the mono-cationic side chains had a stronger cytotoxic activity than compounds **9**, **10**, **13** bearing the di-cationic side chains. An explanation for the lower activity of compounds **9**, **10**, **13** is that these three compounds, because of their higher electrical charge, are less lipophilic and thus more difficult to diffuse through the plasma membrane.

Table 2
IC_{50} cytotoxicity values (μM) of emodin derivatives against tumor cells (data derived from the mean of three independent assays)

Compound	B16	HepG2	LLC
Emodin	> 100	55.1	> 100
6	2.7	2.0	1.7
7	3.6	4.9	4.5
8	1.8	2.7	3.8
9	5.2	5.7	13.1
10	10.1	37.6	12.8
11	6.9	4.9	12.1
12[a]	n.d.	n.d.	n.d.
13	20.1	7.2	8.9

[a] Not determined (n.d.) because of its poor solubility in solvents suitable for the assay.

In conclusion, the new anthrapyrazoles derived from emodin with cationic amino side chains had strong inhibiting activity against various tumor cells, which may be associated with their DNA binding capacity. In particular, the mono-cationic amino side chains introduced into the lead compound appeared to be the major contributors to the DNA binding and cytotoxicity enhancement.

3. Experimental

3.1. Chemistry

Absorbance measurements were performed on a Shimadzu UV-2501 spectrophotometer, and fluorometric measurements were on a Shimadzu RF-5301PC spectrofluorophotometer. Melting points (m.p.) were determined using an X-6 micro-

scope melting point instrument without correction. FAB-MS spectra were obtained using a VG ZAB-HS spectrometer, and ^{1}H NMR spectra and NOESY experiment were performed on a Varian INOVA 500NB with tetramethylsilane (TMS) as an internal standard. Elemental analysis was carried out on an Elementar Vario EL CHNS Elemental Analyzer.

Emodin (purity 98.5%) was extracted from Chinese herb *Polygonum cuspidatum Sieb.et Zucc* according to the method of Kelly et al. [32]. Silica gel F_{254} was used in analytical thin-layer chromatography (TLC) and silica gel H was used in column chromatography.

3.1.1. 1-Hydroxy-6,8-dimethoxy-3-methylanthracene-9,10-dione (2)

To a solution of emodin (**1**) (1.05 g, 3.89 mmol) in dry acetone (105 ml), dimethyl sulfate (1.0 ml) and anhydrous K_2CO_3 (5.0 g) were added and the mixture was stirred for 28 h at 30 °C. The reaction product was evaporated under vacuum and then mixed with water (50 ml). The precipitate was separated from water by filtration and the residue was purified by flash column chromatography with $CHCl_3$ elution. The product was crystallized in acetone, yielding an orange solid as compound **2** (0.70 g, 60%): m.p. 209–212 °C; ^{1}H NMR ($CDCl_3$, 300 MHz): δ 2.43 (s, 3H), 3.98 (s, 3H), 4.02 (s, 3H), 6.76 (d, 1H, $J = 2.4$ Hz), 7.06 (s, 1H), 7.44 (d, 1H, $J = 2.4$ Hz), 7.55 (s, 1H), 13.07 (s, 1H); FAB-MS *m*/*z*: 299 $[M + H]^+$; Anal. Calcd. for $C_{17}H_{14}O_5$: C, 68.45; H, 4.73. Found: C, 68.33; H, 4.76. Compound **2** is the same as that reported previously in [33] as the spectral data are all identical.

3.1.2. 1,3-Dimethoxy-6-methyl-8-[(4-methylphenyl)sulfonyl]oxyanthracene-9,10-dione (3)

To a solution of compound **2** (0.45 g, 1.5 mmol) in dry acetone (200 ml), *p*-toluenesulfonyl chloride (0.57 g 3.0 mmol) and anhydrous K_2CO_3 (4.0 g, 29.0 mmol) were added under nitrogen, and the mixture was refluxed for 5 h. The reaction product was evaporated under vacuum and then mixed with water (100 ml). The precipitate was separated from water by filtration, rinsed with ether (50 ml), and then purified by column chromatography with 70:30 cyclohexane/EtOAc elution to afford a light yellow solid compound **3** (0.58 g, 85%): m.p. 217–219 °C; ^{1}H NMR ($CDCl_3$, 500 MHz): δ 2.38 (s, 3H), 2.46 (s, 3H), 3.94 (s, 3H), 3.95 (s, 3H), 6.74 (d, 1H, $J = 2.5$ Hz), 7.28 (d, 2H, $J = 8.0$ Hz), 7.30 (d, 1H, $J = 2.5$ Hz), 7.41 (d, 1H, $J = 1.0$ Hz), 7.89 (d, 2H, $J = 8.0$ Hz), 7.95 (d, 1H, $J = 1.0$ Hz); FAB-MS *m*/*z*: 453 $[M + H]^+$; Anal. Calcd. for $C_{24}H_{20}O_7S$: C, 63.71; H, 4.45. Found: C, 63.65; H, 4.46.

3.1.3. 2-(2-Hydroxyethyl)-4-methyl-8,10-dimethoxy-anthra[1,9-cd]pyrazol-6(2H)-one (4)

To a solution of compound **3** (0.45 g, 1.0 mmol) in anhydrous 2-ethoxyethanol (20 ml), 2-hydroxyethylhydrazine (0.34 ml, 5.0 mmol) was added and then heated under argon at 120 °C for 4 h. Upon cooling, the mixture was mixed with water (200 ml), and the precipitate was then separated by filtration and washed again with water (50 ml). The residue was purified by column chromatography with cyclohexane/EtOAc (50:50–10:90) elution to afford an orange solid compound **4** (0.19 g, 56%): m.p. 226–228 °C; ^{1}H NMR (DMSO-d_6, 300 MHz): δ 2.59 (s, 3H), 3.85 (q, 2H, $J = 5.1$ Hz), 3.90 (s, 3H), 3.98 (s, 3H), 4.55 (t, 2H, $J = 5.1$ Hz), 4.90 (t, 1H, $J = 4.8$ Hz), 7.01 (d, 1H, $J = 2.4$ Hz), 7.42 (d, 1H, $J = 2.4$ Hz), 7.74 (s, 1H), 7.86 (s, 1H); FAB-MS *m*/*z*: 339 $[M + H]^+$; Anal. Calcd. for $C_{19}H_{18}N_2O_4$: C, 67.44; H, 5.36; N, 8.28. Found: C, 67.28; H,5.43; N, 8.19.

3.1.4. 2-(2-[(Methylsulfonyl)oxy]ethyl)-4-methyl-8,10-dimethoxy-anthra[1,9-cd]pyrazol-6(2H)-one (5)

To a stirred suspension of **4** (0.42 g, 1.00 mmol) and triethylamine (1.0 ml, 7.2 mmol) in dry dichloromethane (75 ml), methanesulfonyl chloride (0.5 ml, 6.46 mmol) was added with cooling at 0 °C. The mixture was then stirred at room temperature for 4 h. The reaction mixture was partitioned between dichloromethane (200 ml) and 1 N sodium hydroxide (20 ml), and the organic phase was washed with HCl (10%, 20 ml), water (20 ml), and finally brine (20 ml), and then concentrated to dryness. The residue was purified by flash chromatography with cyclohexane/EtOAc (50:50–20:80) elution to afford an orange solid compound **5** (0.45 g, 87%): m.p. 242–243 °C; ^{1}H NMR (DMSO-d_6, 300 MHz): δ 2.61 (s, 3H), 3.08 (s, 3H), 3.92 (s, 3H), 4.00 (s, 3H), 4.68 (t, 2H, $J = 4.2$ Hz), 4.88 (t, 2H, $J = 4.2$ Hz), 7.03 (d, 1H, $J = 2.4$ Hz), 7.43 (d, 1H, $J = 2.4$ Hz), 7.78 (s, 1H), 7.90 (s, 1H); FAB-MS *m*/*z*: 417 $[M + H]^+$; Anal. Calcd. for $C_{20}H_{20}N_2O_6S$: C, 57.68; H, 4.84; N, 6.73. Found: C, 57.41; H, 4.90; N, 6.65.

3.1.5. General procedure for the preparation of the amines 6–13

To a stirred solution of compound **5** in anhydrous ethanol, appropriate N,N-dialkylaminoethylamine (20 eq) was added. The mixture was stirred at the reflux temperature for 6–24 h, and then evaporated under vacuum. The residue was purified by column chromatography and elution with $CHCl_3$/MeOH (99:1–80:20). Furthermore, the purified compound was converted into its hydrochloride salt by treatment with excess HCl in ethanol. The precipitate was collected, washed with ethanol, and dried.

3.1.5.1. 2-[2-(Dimethylamino)ethyl]-4-methyl-8,10-dimethoxy-anthra[1,9-cd]pyrazol-6 (2H)-one hydrochloride (6).

An orange solid, yield 80%; m.p. 252–254 °C; ^{1}H NMR (10% D_2O in DMSO-d_6, 300 MHz): δ 2.61 (s, 3H), 2.89 (s, 6H), 3.66 (t, 2H, $J = 6.6$ Hz), 3.91 (s, 3H), 4.01 (s, 3H), 4.98 (t, 2H, $J = 6.6$ Hz), 7.02 (d, 1H, $J = 2.4$ Hz), 7.40 (d, 1H, $J = 2.4$ Hz), 7.77 (s, 1H), 8.00 (s, 1H); FAB-MS *m*/*z*: 366 $[M + H]^+$. Anal. Calcd. for $C_{21}H_{23}N_3O_3 \cdot HCl \cdot 3.4H_2O$: C, 54.46; H, 6.70; N, 9.07. Found: C, 54.74; H, 6.51; N, 9.01.

3.1.5.2. 2-[2-(Diethylamino)ethyl]-4-methyl-8,10-dimethoxy-anthra[1,9-cd]pyrazol- 6(2H)-one hydrochloride (7).

An orange solid, yield 95%; m.p. 230–232 °C; ^{1}H NMR (10%

D_2O in DMSO-d_6, 300 MHz): δ 1.26 (t, 6H, J = 7.0 Hz), 2.62 (s, 3H), 3.29 (q, 4H, J = 7.0 Hz), 3.71 (t, 2H, J = 5.7 Hz), 3.92 (s, 3H), 4.01 (s, 3H), 4.95 (t, 2H, J = 5.7 Hz), 7.03 (d, 1H, J = 2.4 Hz), 7.41 (d, 1H, J = 2.4 Hz), 7.79 (s, 1H), 7.99 (s, 1H); FAB-MS m/z: 394 $[M + H]^+$. Anal. Calcd. for $C_{23}H_{27}N_3O_3 \cdot HCl \cdot 2.1H_2O$: C, 59.06; H, 6.94; N, 8.98. Found: C, 58.88; H, 6.61; N, 8.62.

*3.1.5.3. 2-[2-[(2-Hydroxyethyl)amino]ethyl]-4-methyl-8,10-dimethoxy-anthra[1,9-cd] pyrazol-6(2H)-one hydrochloride (**8**).* An orange solid, yield 80%; m.p. 236–238 °C; ^{1}H NMR (10% D_2O in DMSO-d_6, 300 MHz): δ 2.60 (s, 3H), 3.12 (t, 2H, J = 6.0 Hz), 3.55 (t, 2H, J = 6.0 Hz), 3.66 (t, 2H, J = 6.0 Hz), 3.89 (s, 3H), 3.99 (s, 3H), 4.84 (t, 2H, J = 6.0 Hz), 7.01 (d, 1H, J = 2.4 Hz), 7.40 (d, 1H, J = 2.4 Hz), 7.77 (s, 1H), 7.89 (s, 1H); FAB-MS m/z: 382 $[M + H]^+$. Anal. Calcd. for $C_{21}H_{23}N_3O_4 \cdot HCl \cdot 2.5H_2O$: C, 54.49; H, 6.31; N, 9.08. Found: C, 55.54; H, 6.48; N, 8.80.

*3.1.5.4. 2-[2-[(2-Dimethylaminoethyl)amino]ethyl]-4-methyl-8,10-dimethoxy-anthra [1,9-cd] pyrazol-6(2H)-one hydrochloride (**9**).* An orange solid, yield 81%; m.p. 242–244 °C; ^{1}H NMR (10% D_2O in DMSO-d_6, 300 MHz): δ 2.54 (s, 3H), 2.80 (s, 6H), 3.40 (m, 4H), 3.59 (t, 2H, J = 6.0 Hz), 3.85 (s, 3H), 3.95 (s, 3H), 4.78(t, 2H, J = 6.0 Hz), 6.92 (d, 1H, J = 2.4 Hz), 7.30 (d, 1H, J = 2.4 Hz), 7.67 (s, 1H), 7.80 (s, 1H); FAB-MS m/z: 409 $[M + H]^+$. Anal. Calcd. for $C_{23}H_{28}N_4O_3 \cdot 2HCl \cdot 3H_2O$: C, 51.59; H, 6.78; N, 10.46. Found: C, 51.40; H, 6.74; N, 10.42.

*3.1.5.5. 2-[2-[(2-Diethylaminoethyl)amino]ethyl]-4-methyl-8,10-dimethoxy-anthra [1,9-cd]pyrazol-6(2H)-one hydrochloride (**10**).* An orange solid, yield 85%; m.p. 234–236 °C; ^{1}H NMR (10% D_2O in DMSO-d_6, 300 MHz): δ 1.24 (t, 6H, J = 7.0 Hz), 2.64 (s, 3H), 3.18 (q, 4H, J = 7.0 Hz), 3.41 (m, 4H), 3.67 (t, 2H, J = 4.0 Hz), 3.93 (s, 3H), 4.04 (s, 3H), 4.89 (t, 2H, J = 4.0 Hz), 7.04 (d, 1H, J = 1.8 Hz), 7.44 (d, 1H, J = 1.8 Hz), 7.81 (s, 1H), 7.97 (s, 1H); FAB-MS m/z: 437 $[M + H]^+$. Anal. Calcd. for $C_{25}H_{32}N_4O_3 \cdot 2HCl \cdot 1.2H_2O$: C, 56.54; H, 6.91; N, 10.55. Found: C, 56.49; H, 6.88; N, 10.51.

*3.1.5.6. 2-(2-Piperidin-1-yl-ethyl)-4-methyl-8,10-dimethoxy-anthra[1,9-cd]pyrazol-6(2H)-one hydrochloride (**11**).* A yellow solid, yield 90%; m.p. 260–262 °C; ^{1}H NMR (10% D_2O in DMSO-d_6, 300 MHz): δ 1.93 (m, 6H), 2.63 (s, 3H), 3.06 (t, 2H, J = 6.5 Hz), 3.68 (m, 4H), 3.92 (s, 3H), 4.02 (s, 3H), 4.89 (t, 2H, J = 6.5 Hz), 7.03 (d, 1H, J = 2.5 Hz), 7.42 (d, 1H, J = 2.5 Hz), 7.78 (s, 1H), 7.96 (s, 1H); FAB-MS m/z: 406 $[M + H]^+$. Anal. Calcd. for $C_{24}H_{27}N_3O_3 \cdot HCl \cdot H_2O$: C, 62.67; H, 6.57; N, 9.14. Found: C, 62.38; H, 6.40; N, 9.01.

*3.1.5.7. 2-(2-Morpholinoethyl)-4-methyl-8,10-dimethoxy-anthra[1,9-cd]pyrazol-6(2H)- one hydrochloride (**12**).* An orange solid, yield 91%; m.p. 242–244 °C; ^{1}H NMR (not in hydrochloride form, $CDCl_3$, 300 MHz): δ 2.62 (m, 4H), 2.65 (s, 3H), 3.03 (t, 2H, J = 5.7 Hz), 3.73 (m, 4H),3.97 (s, 3H), 4.10 (s, 3H), 4.69 (t, 2H, J = 5.7 Hz), 6.84 (d, 1H, J = 2.3 Hz), 7.55 (s, 1H), 7.63 (d, 1H, J = 2.3 Hz), 7.88 (s, 1H); FAB-MS m/z: 408 $[M + H]^+$. Anal. Calcd. for $C_{23}H_{25}N_3O_4 \cdot HCl \cdot 1.8H_2O$: C, 57.99; H, 6.26; N, 8.82. Found: C, 58.03; H, 6.01; N, 8.62.

*3.1.5.8. 2-[2-(4-Methylpiperazin-1-yl)ethyl]-4-methyl-8,10-dimethoxy-anthra[1,9-cd] pyrazol-6(2H)-one hydrochloride (**13**).* An orange solid, yield 85%; m.p. 189–190 °C; ^{1}H NMR (not in hydrochloride form, $CDCl_3$, 300 MHz): δ 2.31 (s, 3H), 2.48 (m, 4H), 2.63 (s, 3H), 2.64 (m, 4H), 2.98 (t, 2H, J = 7.0 Hz), 3.95 (s, 3H), 4.08 (s, 3H), 4.62 (t, 2H, J = 7.0 Hz), 6.82 (d, 1H, J = 1.9 Hz), 7.52 (s, 1H), 7.60 (d, 1H, J = 1.9 Hz), 7.86 (s, 1H); FAB-MS m/z: 421 $[M + H]^+$. Anal. Calcd. for $C_{24}H_{28}N_4O_3 \cdot 2HCl \cdot 3H_2O$: C, 52.65; H, 6.63; N, 10.23. Found: C, 52.33; H, 6.66; N, 10.21.

3.2. Spectrometric titration and DNA binding assay

All types of spectrometric titration were conducted in a 1 cm quartz cuvette at room temperature (~30 °C). The CT DNA (Sigma, St. Louis, MO) was dissolved in double distilled deionized water with 50 mM NaCl, and dialyzed against a buffer solution for 2 days. Its concentration was determined by absorption spectrometry at 260 nm using a molar extinction coefficient 6600 M^{-1} cm^{-1}. The ratio $A_{260}/A_{280} > 1.80$ was used as an indication of a protein-free DNA.

Absorption titration was performed at a fixed concentration of drugs (30 μM) in a sodium phosphate buffer (20 mM sodium phosphate, 150 mM NaCl, pH 6.3). Small aliquots of concentrated CT DNA (3.9 mM) were added into the solution at final concentrations from 0 to 165 μM, and stirred for 5 min before measurement. The parameters, λ_{max}, red shift, hypochromicity and isosbestic point were found from the adsorption spectra. Fluorescence titration was performed at a fixed concentration of drugs (3 μM) in sodium phosphate buffer (20 mM sodium phosphate, 20 mM NaCl, pH 6.3). Small aliquots of concentrated CT DNA (3.9 mM) were added into the solution at final concentrations from 0 to 150 μM, and stirred for 5 min. Fluorescence intensity was measured at Ex 410 nm and Ex/Em 10/10 nm. Binding constants were derived from the modified Scatchard equation, $r/C_f = K_i(1 - Nr)[(1 - Nr)/[1 - (N - 1)r]]^{n-1}$, where r is the molar ratio of bound ligand to DNA, C_f the free ligand concentration, K_i the binding constant and n the binding size in base pairs [34].

3.3. Cell cultures and cytotoxicity assay

All tumor cell lines, mouse melanoma B16, human hepatocellular carcinoma HepG2 and LLC cell (from ATCC, Rockville, MD) were cultured on RPMI-1640 medium supplemented with 10% fetal bovine serum, 100 U ml^{-1} penicillin and 100 μg ml^{-1} streptomycin in 25-cm^2 culture flasks at 37 °C in humidified atmosphere with 5% CO_2.

For the cytotoxicity tests, cells in exponential growth stage were harvested from culture by trypsin digestion and centrifuging at 180 × g for 3 min, then resuspended in fresh medium at

a cell density of 5×10^4 cells per ml. The cell suspension was dispensed into a 96-well microplate at 100 μl per well, and incubated in humidified atmosphere with 5% CO_2 at 37 °C for 24 h, and then treated with the compounds at various concentrations (0, 1, 10, 100 μM). After 48 h of treatment, 50 μl of 1 mg ml^{-1} MTT solution was added to each well, and further incubated for 4 h. The cells in each well were then solubilized with DMSO (100 μl for each well) and the optical density (OD) was recorded at 570 nm. All drug doses were tested in triplicate and the IC_{50} values were derived from the mean OD values of the triplicate tests versus drug concentration curves.

Acknowledgements

This work was supported financially by the National Natural Science Foundation of China (20472117), the Science Foundation of Zhuhai (PC20041131), the Guangzhou City and the Guangdong Provincial Science Foundation, and the Hong Kong Polytechnic University through the State Key Lab of Chinese Medicine and Molecular Pharmacology in Shenzhen.

References

[1] S. Alves Daiane, L. Perez-Fons, A. Estepa, V. Micol, Biochem. Pharmacol. 68 (2004) 549–561.
[2] Y.C. Kuo, H.C. Meng, W.J. Tsai, Inflamm. Res. 50 (2001) 73–82.
[3] M.C. Fuzellier, F. Mortier, T. Girard, J. Payen, Ann. Pharm. Fr. 39 (1981) 313–318.
[4] D.L. Barnard, J.H. Huffman, J.L.B. Morris, S.G. Wood, B.G. Hughes, R.W. Sidwell, Antiviral Res. 17 (1992) 63–77.
[5] T.L. Cha, L. Qiu, C.T. Chen, Y. Wen, M.C. Hung, Cancer Res. 65 (2005) 2287–2295.
[6] Y.C. Chen, S.C. Shen, W.R. Lee, F.L. Hsu, H.Y. Lin, C.H. Ko, S.W. Tseng, Biochem. Pharmacol. 64 (2002) 1713–1724.
[7] D.E. Shieh, Y.Y. Chen, M.H. Yen, L.C. Chiang, C.C. Lin, Life Sci. 74 (2004) 2279–2290.
[8] C. Monneret, Eur. J. Med. Chem. 36 (2001) 483–493.
[9] D.E. Graves, L.M. Velea, Curr. Org. Chem. 4 (2000) 915–929.
[10] M.F. Brana, M. Cacho, A. Gradillas, B. De Pascual-Teresa, A. Ramos, Curr. Pharm. Des. 7 (2001) 1745–1780.
[11] L.H. Hurley, Nat. Rev. Cancer 2 (2002) 188–200.
[12] J. Tarasiuk, J. Mazerski, K. Tkaczyk-Gobis, E. Borowski, Eur. J. Med. Chem. 40 (2005) 321–328.
[13] I.R. Judson, Anticancer Drugs 2 (1991) 223–231.
[14] H.D. Showalter, D.W. Fry, W.R. Leopold, J.W. Lown, J.A. Plambeck, K. Reszka, Anticancer Drug Des. 1 (1986) 73–85.
[15] D.W. Fry, Pharmacol. Ther. 52 (1991) 109–125.
[16] L.P. Mai, F. Gueritte, V. Dumontet, M.V. Tri, B. Hill, O. Thoison, D. Guenard, T. Sevenet, J. Nat. Prod. 64 (2001) 1162–1168.
[17] W.M. Cholody, S. Martelli, J. Paradziej-Lukowicz, J. Konopa, J. Med. Chem. 33 (1990) 49–52.
[18] R.K.Y. Zee-Cheng, C.C. Cheng, J. Med. Chem. 21 (1978) 291–294.
[19] R.K.Y. Zee-Cheng, E.G. Podrebarac, C.S. Menon, C.C. Cheng, J. Med. Chem. 22 (1979) 501–505.
[20] J. Feigon, W.A. Denny, W. Leupin, D.R. Kearns, J. Med. Chem. 27 (1984) 450–465.
[21] H.D. Showalter, J.L. Johnson, J.M. Hoftiezer, J. Heterocyclic Chem. 23 (1986) 1491–1501.
[22] A. Oliva, M. Ellis, L. Fiocchi, E. Menta, A.P. Krapcho, J. Heterocyclic Chem. 37 (2000) 47–55.
[23] I.K. Kostakis, P. Magiatis, N. Pouli, P. Marakos, A.L. Skaltsounis, H. Pratsinis, S. Leonce, A. Pierre, J. Med. Chem. 45 (2002) 2599–2609.
[24] W.Y. Zhong, J.S. Yu, W.L. Huang, K. Ni, Y.Q. Liang, Biopolymers 62 (2001) 315–323.
[25] C. Sissi, E. Leo, S. Moro, G. Capranico, A. Mancia, E. Menta, A.P. Krapcho, M. Palumbo, Biochem. Pharmacol. 67 (2004) 631–642.
[26] J.A. Hartley, K. Reszka, E.T. Zuo, W.D. Wilson, A.R. Morgan, J.W. Lown, Mol. Pharmacol. 33 (1988) 265–271.
[27] H.M. Berman, P.R. Young, Annu. Rev. Biophys. Bioeng. 10 (1981) 87–114.
[28] H. Ihmels, K. Faulhaber, G. Viola, Evaluation of the DNA-binding properties of cationic dyes by absorption and emission spectroscopy, in: C. Schmuck, H. Wennemers (Eds.), Highlights in Bioorganic Chemistry: Methods and Applications, Wiley-VCH, Weinheim, 2004.
[29] E.C. Long, J.K. Barton, Acc. Chem. Res. 23 (1990) 271–273.
[30] J.Y. Pang, Y. Qin, W.H. Chen, G.A. Luo, Z.H. Jiang, Bioorg. Med. Chem. 13 (2005) 5835–5840.
[31] W.A. Denny, G.J. Atwell, B.C. Baguley, L.P.G. Wakelin, J. Med. Chem. 28 (1985) 1568–1574.
[32] T.R. Kelly, N.S. Chandrakumar, N. Walters, J. Blancaflor, J. Org. Chem. 48 (1983) 3573–3574.
[33] J. Banville, J.L. Grandmaison, G. Lang, P. Brassard, Can. J. Chem. 52 (1974) 80–87.
[34] J.D. McGhee, P.H. Von Hippel, J. Mol. Biol. 86 (1974) 469–489.